Template-guided Functional Network Identification via Supervised Dictionary Learning

Yu Zhao[1], Xiang Li[2], Milad Makkie[1], Shannon Quinn[1], Binbin Lin[3], Jieping Ye[3], Tianming Liu[1]

[1]Department of Computer Science, University of Georgia, Athens, GA; [2]Department of Radiology, Massachusetts General Hospital, Boston, MA; [3]Department of Computational Medicine and Bioinformatics, University of Michigan, Ann Arbor, MI

ABSTRACT

Functional network analysis based on matrix decomposition/factorization methods including ICA and dictionary learning models have become a popular approach in fMRI study. Yet it is still a challenging issue in interpreting the result networks because of the inter-subject variability and image noises, thus in many cases, manual inspection on the obtained networks is needed. Aiming to provide a fast and reliable functional network identification tool for both normal and diseased brain fMRI data analysis, in this work, we propose a novel supervised dictionary learning model based on rank-1 matrix decomposition algorithm (S-r1DL) with sparseness constraint. Application on the Autism Brain Imaging Data Exchange (ABIDE) database showed that S-r1DL can fast and accurately identify the functional networks based on the given templates, comparing to unsupervised learning method.

Index Terms—functional network identification, supervised learning, autism spectrum disorder(ASD), network based diagnosis

1. INTRODUCTION

In recent functional neuroimaging studies, matrix decomposition-based data driven methods have been widely applied, including Independent Component Analysis (ICA) [1] and dictionary learning [2] [3]. The main purpose of these methods is to discover and reconstruct the intrinsic functional organization patterns, modeled by "functional networks", from fMRI data. Such functional networks are defined by a collection of brain regions with specific temporal/spatial properties (e.g. in dictionary learning, the spatial maps of those regions are constrained by sparseness), and are used to characterizes the brain's functional aggregation behavior into neuroscientifically meaningful atomic elements. A series of important functional networks have been discovered by these methods in literatures, including the Default Mode Network (DMN) and other well-established resting-state networks (RSNs) [4]. However, the identification procedure of the functional networks from a given individual dataset is not trivial. It is still a great challenge to identify a functional network that is corresponding to the pre-defined spatial template (e.g. DMN) from the decomposition results. Faced with the vast diversity within the individual brains and their decomposed functional networks, visual inspection or manual check have been typically adopted for accurate network identification [5], in addition to the template matching based on spatial map similarities. Several automatic approaches were developed incorporating temporal and spatial patterns from paradigm templates to identify corresponding networks [6]–[8]. Advanced techniques employing machine learning algorithms were also applied for network identifications by using representing networks in multi-dimensional space as signatures [9]. Yet most of the current works for network identification are training-based, thus the performance is depended on the (usually limited) data availability. In addition, the machine learning methods often add another layer of complexity into the decomposition model, leading to increased time cost and decreased robustness. Therefore, a fast and robust pattern-specific functional network identification modeling is highly demanded for supporting the high-throughput neuroimaging bigdata analytics and aiding the clinical diagnosis of brain disorders based on functional brain imaging data.

One of the popular applications of network-based analysis on diagnosis purposes is on the Autism Spectrum Disorder (ASD) datasets, which has gained great interest from research communities to obtain insights on the causes and find potential treatments. Many analytical techniques have been developed for analyzing the fMRI data from ASD subjects. Functional abnormalities involved in multiple anatomical regions have been discovered [10]. Region of interest (ROI), seed-based correlation techniques were developed to analyze the connectivity of specific brain networks [11], [12]. However, seed ROI selections have a huge influence on the analysis results, which may invoke investigator-specific (seed size or location) or subject-specific (different functional localization) problems [13]. ICA methods have been applied to identify patterns of the underlying signal sources [1], uncovering the spontaneous activity of the human brain [14]. But as mentioned above, separating physiological noise components from the 'true' neural components or identifying specific functional networks are challenging for explaining

978-1-5090-1172-8/17/$31.00 ©2017 IEEE

Authorized licensed use limited to: Harvard Library. Downloaded on March 25,2021 at 17:38:16 UTC from IEEE Xplore. Restrictions apply.

the ICA results [15], thus limit its potential applicability in ASD data analysis.

Inspired by many flexible frameworks that can supervise the learning procedure with neuroscience knowledge [16], [17], and recognizing the needs for a fast functional network identification tool and based on the previous success in using dictionary learning for fMRI analysis [3], in this work, we proposed a supervised dictionary learning model guided by the pre-defined templates. The model extended the scalable fast rank-1 dictionary Learning (r1DL) [18] by simply and efficiently initializing rows of coefficient matrix as template networks (TN), aiming to discover the functional network from the massive voxel-wise fMRI data correspondent to the template using a fast rank-1 matrix decomposition algorithm. The model results on the Autism Brain Imaging Data Exchange (ABIDE) database show that S-r1DL can fast and accurately identify the functional networks based on the 5 templates related with ASD dysfunctional abnormities.

2. MATERIALS AND METHODS

2.1. Supervised Dictionary Learning based on Rank-1 Decomposition

I In this work we used the resting-state fMRI (rsfMRI) data from the Autism Brain Imaging Data Exchange (ABIDE) database [19]. The rsfMRI data were collected from 79 ASD patients and 105 normal controls from NYU Langone Medical Center. The acquisition parameters were as follows: 240mm FOV, 33 slices, TR=2s, TE=15ms, flip angle=90°, scan time=6mins, voxel size=3×3×4mm. In order to have a balanced dataset for the later classification analysis, we used 78 subjects from patients and 78 subjects from normal controls. Data preprocessing includes motion correction, spatial smoothing, temporal pre-whitening, slice time correction, global drift removal, and linear registration to the MNI space.

We used 5 network templates for the supervise dictionary learning which are reported with ASD-related dysfunctional abnormalities in literatures [10]. These templates include regions of: 1) Fusiform Gyrus, which has been reported with hypoactive in ASD patients [10]; 2) Inferior Frontal Gyrus (IFG), the left part of IFG was reported to have decreased activation in ASDs compared to controls ; 3) Anterior Cingulate Cortex (ACC), which has been reported to have decreased activation in adults with autism [20]; 4) Posterior Cingulate Cortex (PCC), where significantly lower connectivity was reported in ASDs during resting state [21]. In addition, Default Mode Network (DMN) has also been examined and discussed by enormous ASD researches [22]. Templates defining the 4 brain regions were extracted from the Harvard-Oxford atlas [23], templates defining the DMN was obtained by the group-wise Independent Component Analysis (ICA) [4].

2.2. Data Acquisition and Pre-processing

In this work, the functional network decomposition and identification is achieved by supervised rank-1 dictionary learning method, by extending the data-driven rank-1 dictionary learning algorithm [18]. Given the input data matrix S of dimension T×P, where for fMRI data T is the temporal length measured in volumes and P is the total number of voxels, we aim to learn a series of basis vector pairs [u, v] from S with the following energy function:

$$L(u,v) = \|S - uv^T\|_F, \text{s.t.}\, \|u\| = 1, \|v\|_0 \le r. \quad (1)$$

Eq. 1 indicates that u and v are supposed to span (i.e. outer product) a rank-1 matrix which approximates S, while at the same time the total number of non-zero elements in v is smaller or equal to the pre-defined sparsity constraint r. The minimization of Eq. 1 is followed by the alternative updating of u and v. Given vector v as constant, the estimation of vector u is just a matrix-vector multiplication:

$$u = \underset{u}{\operatorname{argmin}} \|S - uv^T\|_F = \frac{Sv}{\|Sv\|}. \quad (2)$$

While given vector u as constant, the estimation of vector v involves vector-matrix multiplication and a vector partitioning to find the r number of largest elements in v:

$$v = \underset{v}{\operatorname{argmin}} \|S - uv^T\|_F, s.t. \|v\|_0 \le r. \quad (3)$$

The alternative updating is finshed when the results have converged:

$$\left\|u^{j+1} - u^j\right\| < \varepsilon, \varepsilon = 0.01. \quad (4)$$

In the analysis of fMRI data, u which is a T×1 vector characterize the temporal pattern of the decomposed functional network over a total of T time points, while v which is a P×1 vector characterize the spatial pattern of the network over the P number of voxels.

As we are also aiming for identifying the network that resembles the given spatial template defined in the P×1 vector TN (or the absence of that template network from the data), the estimated v representing the spatial pattern is supposed to be as similar to TN as possible, thus extending the above rank-1 dictionary learning to the supervised rank-1 dictionary learning (S-r1DL) framework. There exist various methods in supervising the learning process and pulling the updating of v towards TN. Based on preliminary studies we found that simply initializing v as TN could work well for the network identification purpose. Also, the initialization strategy has advantages over other supervised learning methods as its results are the most faithful representation of the input data. Specifically, before the updating loop v is set to TN before starting the estimation of u in the updating loop. The result v is compared with TN based on the spatial overlap rate (SOR):

$$S(v, TN) = \frac{\sum_{i=1}^{P} min(v_i, TN_i)}{\sum_{i=1}^{P} (v_i + TN_i)/2} \quad (5)$$

Authorized licensed use limited to: Harvard Library. Downloaded on March 25,2021 at 17:38:16 UTC from IEEE Xplore. Restrictions apply.

which is the ratio of the sum of the minimum value in each of the i-th voxel over the summation of the averaged values of each i-th voxel of network defined in v and template defined in TN. We then determine whether the network has been identified based on the SOR using an empirically-determined threshold of 0.2. SOR value smaller than 0.2 indicates that supervised learning result deviates too far from the initialization thus the template network could not be identified from the data S. After identifying the first functional network, the algorithm will deflate the input matrix S to its residual R by subtracting from the rank-1 matrix spanned by [u, v]:

$$R^n = R^{n-1} - uv^T, R^0 = S, 1 < n \leq K, \qquad (6)$$

then learn the next pair of dictionary basis following steps described in Eq. 2~4, to the total number of K dictionaries. The learning of the consequent dictionaries can be supervised (using another TN) or unsupervised where the vector u is initialized by randomly selecting one signal from R. In this study, we perform the network identification individually for each template. Thus for one input data S we will perform the learning individually for 5 times (as we are using 5 templates). The algorithm pipeline of the S-r1DL framework using one template is illustrated in Fig. 1(a).

For comparison, we also tested the performance of unsupervised dictionary learning. In order to identify the functional networks correspondent to the template TN from the learning results, we calculated the SOR value between TN and each of the network using Eq. 5, then selected the network with the maximum SOR value. This method has been used extensively for the network-based analysis both in our previous studies and in various literatures [24]. The algorithm pipeline of the unsupervised r1DL framework for functional network identification is illustrated in Fig. 1(b).

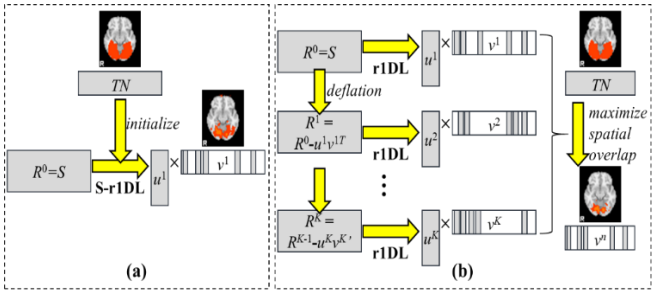

Figure 1. (a) Illustration of the algorithm pipeline of the S-r1DL model with the visualization of the spatial maps of one sample template network (marked as "TN") and the result network defined in v1. (b) Illustration of the alternative strategy based on the unsupervised r1DL model. The same template network is visualized as "TN". The identified network based on spatial overlap method is defined in vn and also visualized.

3. EXPERIMENTAL RESULTS

3.1. Functional network identification result based on 5 templates

By performing the S-r1DL on the rsfMRI data of 156 subjects (78 normal controls, 78 patients) from the ABIDE dataset using 5 templates, we identified the corresponding 5 functional networks (or the absence of them) on each subject. An illustration showing the network identification result of one sample subject is shown in Fig. 2 below.

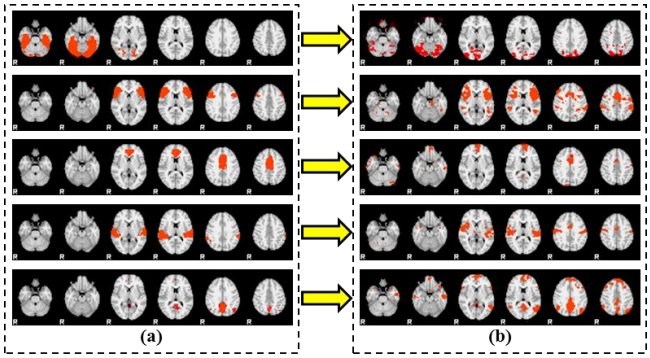

Figure 2. (a) Visualization of the 5 template networks (from top to bottom): Fusiform, IFG, ACC, PCC and DMN. (b) Visualization of the functional networks identified by the S-r1DL method based on the 5 templates.

On the other hand, we have observed substantial variations among the spatial patterns of the identified functional networks across different subjects. Taken Fusiform Gyrus as an example, this network was identified (with SOR value greater than 0.2) from 23 normal control subjects and 34 patient subjects out of the total 156 subjects. The spatial patterns of all the networks are summarized in Fig. 3, showing that individual results are highly deviated, but still capable of being identified by the S-r1DL model. The number of subjects with the identified functional networks correspondent to the 5 templates are listed in Table. 1, showing consistent observation with the literature reports regarding the hyper/lower activities in these regions except the DMN. As in our study it was found that DMN could be recovered as one of the most dominant networks from almost all the subjects regardless of their group.

Table. 1. Number of subjects (out of 78) in each of the normal control (NC) and ASD patient group with the identified functional networks based on the 5 templates. Results from S-r1DL are listed in the top two rows, results from unsupervised r1DL are listed in the bottom two rows.

Method	Group	Fusiform	IFG	ACC	PCC	DMN
S-r1DL	NC	23	56	64	48	78
	Patient	34	47	63	36	73
r1DL	NC	17	52	53	45	78
	Patient	22	48	60	31	77

Authorized licensed use limited to: Harvard Library. Downloaded on March 25,2021 at 17:38:16 UTC from IEEE Xplore. Restrictions apply.

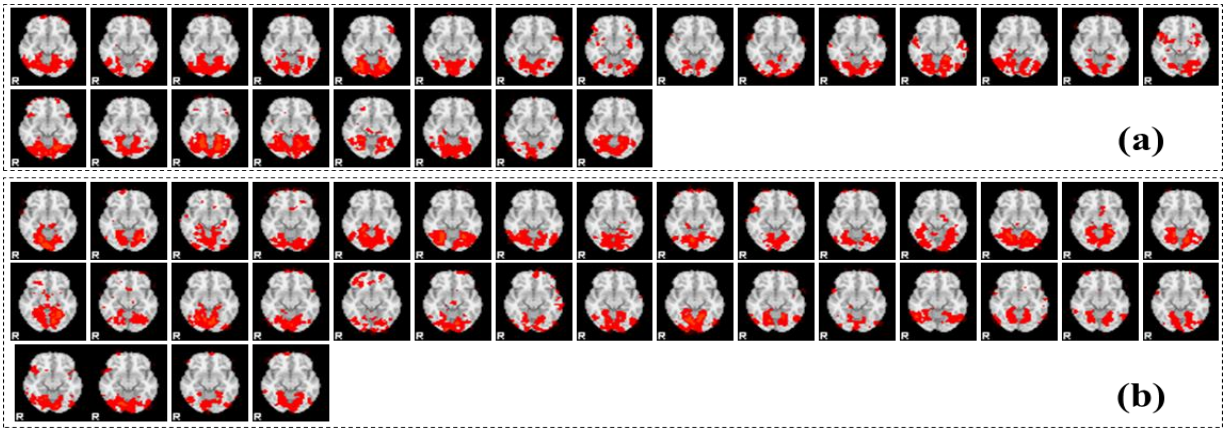

Figure 3. Visualization of the (a) 23 functional networks identified from normal control, and (b) 34 functional networks from ASD patient subjects based on the Fusiform Gyrus template.

3.2. Performance comparison between supervised and unsupervised learning

For comparison, we have also performed the unsupervised dictionary learning by r1DL on the same dataset using K=100 which supposed to be large enough to cover all the potential functional networks during resting-state. The correspondent functional networks based on the 5 templates were then identified by the SOR maximization method described in 2.1. Results from the unsupervised learning show that most of the functional networks identified by the S-r1DL can be found in the 100 networks learned by r1DL (with SOR value greater than 0.2), as listed in Table. 1. The spatial patterns of the identified functional networks by the two methods are also very similar, with the average SOR value greater than 0.7. The consistent results from the supervised and unsupervised learning validates the accuracy of the S-r1DL, showing that the supervised learning process was not biased towards the template.

However, it is worth noting that the time cost for analyzing one subject using one template is only around 2 seconds by S-r1DL. Thus for analyzing the whole group of ABIDE dataset, it only took around 6 minutes to finish the network identification of one template. On the other hand, as we need to learn all the 100 functional networks from each individual dataset using the unsupervised learning and calculate their SOR value with the template, the time cost is much greater. It would take more than 10 minutes to analyze one subject using one template, and around 30 hours to finish the analysis on the whole group of data.

4. CONCLUSION

In this work we proposed the supervised dictionary learning model based on rank-1 matrix decomposition aiming at identifying functional networks from fMRI data based on pre-defined network templates. While we have observed differences in the networks identified from normal control and patient subjects, we are still investigating the intrinsic alterations in the spatial patterns that causing such difference at individual level. More detailed analysis of the identification process including study on decomposition residuals would be needed before we can perform effective and accurate diagnosis based on the functional network identification results. Another important issue we are trying to address in the ongoing work is on the large spatial variations of the functional networks across individuals which has been observed in the results. Such large variability will decrease the accuracy of the spatial similarity measurements (e.g. the SOR used in this work). In that sense, traditional network identification methods including manual inspection which is similar to the unsupervised learning scheme used in this work could be suffered from the inaccurate template matching caused by inter-subjects variability and registration. While S-r1DL has been shown to be capable of recovering the highly deviated functional networks, we are developing algorithms to re-align the identification results in order to enable more accurate comparisons.

5. REFERENCES

[1] M. J. McKeown, S. Makeig, G. G. Brown, T. P. Jung, S. S. Kindermann, A. J. Bell, and T. J. Sejnowski, “Analysis of fMRI data by blind separation into independent spatial components,” *Hum. Brain Mapp.*, vol. 6, no. 3, pp. 160–188, Jan. 1998.

[2] Y.-B. Lee, J. Lee, S. Tak, K. Lee, D. L. Na, S. W. Seo, Y. Jeong, and J. C. Ye, “Sparse SPM: Group Sparse-dictionary learning in SPM framework for resting-state functional connectivity MRI analysis,” *Neuroimage*, vol. 125, pp. 1032–1045, 2016.

[3] J. Lv, X. Jiang, X. Li, D. Zhu, S. Zhang, S. Zhao, H. Chen, T. Zhang, X. Hu, J. Han, J. Ye, L. Guo, and T. Liu, “Holistic atlases of functional networks and interactions reveal reciprocal organizational architecture of cortical function.,” *IEEE Trans. Biomed. Eng.*, vol. 62, no. 4, pp. 1120–31, Apr. 2015.

[4] S. M. Smith, P. T. Fox, K. L. Miller, D. C. Glahn, P. M. Fox, C. E. Mackay, N. Filippini, K. E. Watkins, R. Toro, A. R. Laird,

Authorized licensed use limited to: Harvard Library. Downloaded on March 25,2021 at 17:38:16 UTC from IEEE Xplore. Restrictions apply.

and C. F. Beckmann, “Correspondence of the brain’s functional architecture during activation and rest.,” *Proc. Natl. Acad. Sci. U. S. A.*, vol. 106, no. 31, pp. 13040–5, Aug. 2009.

[5] R. E. Kelly, G. S. Alexopoulos, Z. Wang, F. M. Gunning, C. F. Murphy, S. S. Morimoto, D. Kanellopoulos, Z. Jia, K. O. Lim, and M. J. Hoptman, “Visual inspection of independent components: defining a procedure for artifact removal from fMRI data.,” *J. Neurosci. Methods*, vol. 189, no. 2, pp. 233–45, Jun. 2010.

[6] V. D. Calhoun, T. Adali, M. C. Stevens, K. A. Kiehl, and J. J. Pekar, “Semi-blind ICA of fMRI: A method for utilizing hypothesis-derived time courses in a spatial ICA analysis,” *Neuroimage*, vol. 25, no. 2, pp. 527–538, 2005.

[7] V. D. Calhoun, P. K. Maciejewski, G. D. Pearlson, and K. A. Kiehl, “Temporal lobe and "default" hemodynamic brain modes discriminate between schizophrenia and bipolar disorder.,” *Hum. Brain Mapp.*, vol. 29, no. 11, pp. 1265–75, Nov. 2008.

[8] V. Perlbarg, P. Bellec, J.-L. Anton, M. Pélégrini-Issac, J. Doyon, and H. Benali, “CORSICA: correction of structured noise in fMRI by automatic identification of ICA components.,” *Magn. Reson. Imaging*, vol. 25, no. 1, pp. 35–46, Jan. 2007.

[9] F. De Martino, F. Gentile, F. Esposito, M. Balsi, F. Di Salle, R. Goebel, and E. Formisano, “Classification of fMRI independent components using IC-fingerprints and support vector machine classifiers,” *Neuroimage*, vol. 34, no. 1, pp. 177–194, 2007.

[10] K. A. Stigler, B. C. McDonald, A. Anand, A. J. Saykin, and C. J. McDougle, “Structural and functional magnetic resonance imaging of autism spectrum disorders.,” *Brain Res.*, vol. 1380, pp. 146–61, Mar. 2011.

[11] D. P. Kennedy and E. Courchesne, “Functional abnormalities of the default network during self- and other-reflection in autism.,” *Soc. Cogn. Affect. Neurosci.*, vol. 3, no. 2, pp. 177–90, Jun. 2008.

[12] C. S. Monk, S. J. Peltier, J. L. Wiggins, S.-J. Weng, M. Carrasco, S. Risi, and C. Lord, “Abnormalities of intrinsic functional connectivity in autism spectrum disorders.,” *Neuroimage*, vol. 47, no. 2, pp. 764–72, Aug. 2009.

[13] D. M. Cole, S. M. Smith, and C. F. Beckmann, “Advances and pitfalls in the analysis and interpretation of resting-state FMRI data.,” *Front. Syst. Neurosci.*, vol. 4, p. 8, 2010.

[14] V. Kiviniemi, T. Starck, J. Remes, X. Long, J. Nikkinen, M. Haapea, J. Veijola, I. Moilanen, M. Isohanni, Y.-F. Zang, and O. Tervonen, “Functional segmentation of the brain cortex using high model order group PICA.,” *Hum. Brain Mapp.*, vol. 30, no. 12, pp. 3865–86, Dec. 2009.

[15] J. Tohka, K. Foerde, A. R. Aron, S. M. Tom, A. W. Toga, and R. A. Poldrack, “Automatic independent component labeling for artifact removal in fMRI.,” *Neuroimage*, vol. 39, no. 3, pp. 1227–45, Feb. 2008.

[16] J. Lv, B. Lin, W. Zhang, X. Jiang, X. Hu, J. Han, L. Guo, J. Ye, and T. Liu, “Modeling Task FMRI Data via Supervised Stochastic Coordinate Coding,” Springer International Publishing, 2015, pp. 239–246.

[17] S. Zhao, J. Han, J. Lv, X. Jiang, X. Hu, Y. Zhao, B. Ge, L. Guo, and T. Liu, “Supervised Dictionary Learning for Inferring Concurrent Brain Networks,” *IEEE Trans. Med. Imaging*, vol. 34, no. 10, pp. 2036–2045, Oct. 2015.

[18] X. Li, M. Makkie, B. Lin, M. Sedigh Fazli, I. Davidson, J. Ye, T. Liu, and S. Quinn, “Scalable Fast Rank-1 Dictionary Learning for fMRI Big Data Analysis.”

[19] “http://fcon_1000.projects.nitrc.org/indi/abide/.” .

[20] R. Showcase, @ Cmu, R. K. Kana, T. A. Keller, N. J. Minshew, and M. A. Just, “Inhibitory control in high functioning autism: Decreased activation and underconnectivity in inhibition networks Inhibitory Control in High-Functioning Autism: Decreased Activation and Underconnectivity in Inhibition Networks,” *Biol. Psychiatry*, pp. 198–206, 2007.

[21] V. L. Cherkassky, R. K. Kana, T. A. Keller, and M. A. Just, “Functional connectivity in a baseline resting-state network in autism.,” *Neuroreport*, vol. 17, no. 16, pp. 1687–90, Nov. 2006.

[22] R. K. Kana, L. Q. Uddin, T. Kenet, D. Chugani, and R.-A. MÃ¼ller, “Brain connectivity in autism,” *Front. Hum. Neurosci.*, vol. 8, p. 349, Jun. 2014.

[23] “http://neuro.imm.dtu.dk/wiki/Harvard-Oxford_Atlas.” .

[24] Z. Wang and B. S. Peterson, “Partner-matching for the automated identification of reproducible ICA components from fMRI datasets: algorithm and validation.,” *Hum. Brain Mapp.*, vol. 29, no. 8, pp. 875–93, Aug. 2008.

Authorized licensed use limited to: Harvard Library. Downloaded on March 25,2021 at 17:38:16 UTC from IEEE Xplore. Restrictions apply.